Lévy noises: Double stochastic resonance in a single-well potential

Bartłomiej Dybiec*
Marian Smoluchowski Institute of Physics, and Mark Kac Center for Complex Systems Research, Jagellonian University, ul. Reymonta 4, 30-059 Kraków, Poland

(Received 30 June 2009; revised manuscript received 23 August 2009; published 7 October 2009)

We study properties of a single-well fourth-order potential perturbed by a periodically modulated stable noise. Periodic modulation of the stable noise asymmetry results in an occurrence of the dynamical hysteresis which is the manifestation of the stochastic resonance in the system at hand. We show that the single-well potential with time modulated stable driving is a minimalistic setup, allowing the occurrence of the stochastic resonance (as measured by the hysteresis loop area). Finally, we demonstrate that the observed stochastic resonance is of the double type, i.e., the system efficiency measured by the hysteresis loop area depends in a nonmonotonous way both on the scale parameter (noise intensity) and on the stability exponent characterizing tails asymptotic of noise pulses.

DOI: 10.1103/PhysRevE.80.041111 PACS number(s): 05.40.Fb, 05.10.Gg, 02.50.Ey

I. INTRODUCTION AND MOTIVATION

In the theory of dynamical systems noise serves as a standard description of the system's interactions with the environment. Noise mimics interactions which are unknown or not fully known. In the simplest situations, it is assumed that noise is white and Gaussian. The whiteness of noise means that interactions have an independent character. Gaussianity of noise appears as a consequence of bounded type of interactions. In situations far from the equilibrium, due to strong interactions with the surroundings, the Gaussianity of the noisy term can be violated. However, interactions still can be of the white type. Lévy stable noise, because of its heavy-tail characteristics and infinite divisibility [1,2], can be used to describe interactions which go beyond the equilibrium, Gaussian realms [3,4].

The growing experimental evidence suggests that there is a need to consider a more general type of noises than Gaussian. The manifestation of a more general heavy-tailed fluctuations has been observed in various situations ranging from the description of the dynamics in plasmas, diffusion in the energy space [5], exciton and charge transport in polymers under conformational motion [6] and incoherent atomic radiation trapping [4,7,8] to the spectral analysis of paleoclimatic [9,10] or economic data [11], motion in optimal search strategies among randomly distributed target sites [12,13] (with some level of controversy [14]), fluorophore diffusion as studied in photobleaching experiments [15], two-dimensional rotating flow [16], and many others. The area of applicability of Lévy stable noises is steadily growing over time including noise-induced effects [17–22], game theory [23,24], economics [25], medicine [26], epidemiology [27,28], ecology [29], and many others [4].

The presence of noise in physical systems underlines the occurrence of noise-induced effects. Among noise-induced effects manifesting constructive role of noises there are stochastic resonance [30,31], stochastic multiresonance [32–34], resonant activation [35,36], stochastic synchronization [37,38], and noise-enhanced stability [39]. The presence of a certain amount of noise is indispensable to observe the abovementioned effects. Here, we focus on the examination of the dynamical hysteresis and the stochastic resonance in a system driven by time-dependent white Lévy noise.

II. METHODS AND RESULTS

Stochastic resonance is a noise-induced effect demonstrating the possibility of a signal amplification. In stochastic resonance, the weak input signal due to the presence of a stochastic component in the system dynamic is amplified and consequently detectable. An analysis of the stochastic resonance [30,31] is based on appropriate measures. These measures depend in a nonmonotonous way on the noise intensity [30,31]. An increase in the noise intensity to a certain optimal level improves the output signal quality as measured by the signal-to-noise ratio (SNR), spectral power amplification, residence time distribution [40,41], probability of a given number of transitions per period of an external driving [42], or the dynamical hysteresis loop area [22,43,44]. Stochastic resonance is a common effect manifesting the constructive role of noises. Among others, stochastic resonance was experimentally observed in digital devices such as Schmitt triggers [37], ring lasers [45], vertical cavity surface emitting lasers [46], or colloidal suspensions [47]. Biological systems also display characteristic features of stochastic resonance [48–52].

The periodic modulation of a bistable potential, due to a time delayed response of the system to the external stimulus, results in the effect of the dynamical hysteresis [53,54]. The hysteresis loop area is sensitive to the noise [19] and system parameters [22,54–57] and can be used as a measure of the stochastic resonance. Furthermore, it can be used as a quantity measuring input-output synchronization [53,54,56].

Contrary to traditional modeling of the stochastic resonance, we demonstrate that a single-well fourth-order potential accompanied with time-dependent noise, more general than Gaussian, is sufficient to produce stochastic resonance (as measured by the hysteresis loop area). Furthermore, we show that the system response has a nonmonotonous depen-

*bartek@th.if.uj.edu.pl

dence not only as a function of a noise intensity but also as a function of the stability index α describing a heavy-tail character of stable noise pulses. The nonmonotonous dependence of the hysteresis loop area as a function of two noise parameters (scale parameter and stability index) makes the observed stochastic resonance of the double type. The double resonance, observed here, differs from the stochastic multiresonance [32,34] where a variation in a single parameter leads to multiple maxima of a resonance quantifier.

The current researches extend earlier studies on the stochastic resonance induced by α-stable noises [19,22] by limiting the number of required assumptions. Traditionally, a periodically modulated double-well potential provides the model system for occurrence of the stochastic resonance. In [22] the influence of α-stable noises on the stochastic resonance in the periodically modulated double-well potential was inspected. Here, it will be demonstrated that periodically modulated double-well potential is not indispensable for the occurrence of the stochastic resonance. In contrast to the double-well potential, it is possible to find an alternative minimalistic setup leading to the occurrence of the dynamical hysteresis [19]. The α-stable noise with a periodically modulated asymmetry parameter is sufficient to result in the stochastic resonance (as measured by the hysteresis loop area) in the single-well potential. The findings presented in the following sections extend existing studies on the role of Lévy flights in physical systems [17,18,20–22].

A. Methods

The studied system is modeled by the overdamped Langevin equation driven by a white Lévy noise

$$\dot{x}(t) = -V'(x) + \zeta(t). \tag{1}$$

$\zeta(t)$ represents white Lévy noise and $V(x)$ stands for the fourth-order single-well potential

$$V(x) = \frac{x^4}{4}. \tag{2}$$

In the free case, i.e., $V(x)=0$, the Lévy noise leads to the increments which are distributed according to a α-stable density whose characteristic function $[\phi(k) = \int_{-\infty}^{\infty} e^{ikx} l_{\alpha,\beta}(x;\sigma,\mu)dx]$ for $\alpha \neq 1$ [1,2] is

$$\phi(k) = \exp\left[-\sigma^{\alpha}|k|^{\alpha}\left(1 - i\beta\,\mathrm{sgn}(k)\tan\frac{\pi\alpha}{2}\right) + i\mu k\right], \tag{3}$$

while for $\alpha=1$ it is

$$\phi(k) = \exp\left[-\sigma|k|\left(1 + i\beta\frac{2}{\pi}\mathrm{sgn}(k)\ln|k|\right) + i\mu k\right]. \tag{4}$$

Stable densities are characterized by four parameters: the stability index α $\{\alpha \in (0,2]\}$, the asymmetry parameter β $(\beta \in [-1,1])$, the scale parameter σ $(\sigma > 0)$, and the location parameter μ $(\mu \in \mathbb{R})$. The stability index α describes the asymptotic behavior of stable densities, i.e., for a large x stable densities are characterized by a power-law tail of $|x|^{-(\alpha+1)}$ type. The asymmetry parameter β characterizes the skewness of the distribution [1,2], i.e.,

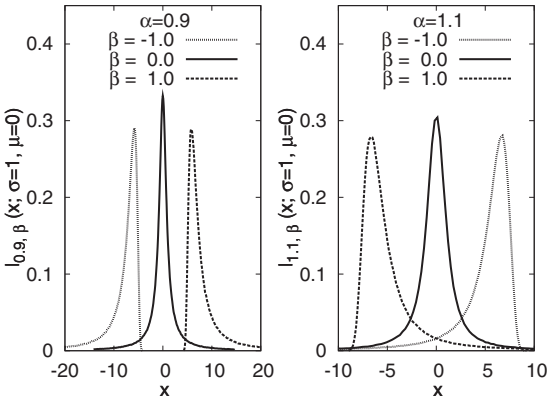

FIG. 1. Sample stable densities with $\alpha=0.9$ (left panel) and $\alpha=1.1$ (right panel). For $\beta=0$ distributions are symmetric and become asymmetric for $\beta \neq 0$. The support of the densities for the fully asymmetric cases with $\beta=\pm 1$ and $\alpha<1$ (left panel) assumes only negative values for $\beta=-1$ and only positive values for $\beta=1$. Note the differences in the positions of the maxima for $\alpha<1$ and $\alpha>1$.

$$\lim_{x\to\infty}\frac{\mathrm{Prob}(X>x)}{\mathrm{Prob}(|X|>x)} = \frac{1+\beta}{2}. \tag{5}$$

In particular, for $\beta=0$ stable densities are symmetric ones. The location parameter μ determines the location of the modal value. Finally, σ describes the overall distribution width. The case $\alpha=2$ with any value of β corresponds to the Gaussian density. In such a case, μ represents the mean value and σ stands for the standard deviation. Stable densities generalize the Gaussian distribution in the sense in which the generalized central limit theorem generalizes the standard central limit theorem [58]. Systems driven by white α-stable noises reconstruct their Gaussian counterparts in the limit of $\alpha=2$. Figure 1 presents sample stable densities for $\alpha=0.9$ (left panel) and $\alpha=1.1$ (right panel) with various asymmetry parameters β.

The position of the Brownian particle subjected to additive white Lévy noise is calculated by direct integration of Eq. (1) with respect to the α-stable measure [1,2,59–64],

$$x(t+\Delta t) = x(t) - V'(x(t))\Delta t + (\Delta t)^{1/\alpha}\zeta, \tag{6}$$

where ζ is distributed according to the α-stable Lévy-type distribution $l_{\alpha,\beta}(\zeta;\sigma,\mu=0)$ whose representation [1,2] is given by the characteristic function $\phi(k)$ [see Eqs. (3) and (4)].

The Langevin equation (1) describes the system's evolution on the trajectory level. The fractional Fokker-Planck equation [65–70] describes the evolution of the probability density function. For $\alpha \neq 1$, the fractional Fokker-Planck equation associated with the Langevin equation (1) has the form [65–70]

$$\frac{\partial p(x,t)}{\partial t} = \frac{\partial}{\partial x}[V'(x,t) - \mu]p(x,t) + \sigma^{\alpha}\frac{\partial^{\alpha}}{\partial|x|^{\alpha}}p(x,t) + \sigma^{\alpha}\beta\tan\frac{\pi\alpha}{2}\frac{\partial}{\partial x}\frac{\partial^{\alpha-1}}{\partial|x|^{\alpha-1}}p(x,t). \tag{7}$$

The fractional (space) Riesz-Weyl derivative [71] is understood in the Fourier transform sense

$$\mathcal{F}\left[\frac{\partial^{\alpha}}{\partial|x|^{\alpha}}p(x,t)\right] = -|k|^{\alpha}\hat{p}(k,t). \tag{8}$$

The fractional derivative is nonlocal in space which captures the possibility of anomalously long jumps [see Eqs. (3) and (4)].

The fourth-order potential is sufficient to produce bounded stationary states [17,72,73], i.e., states characterized by the finite variance, even for asymmetric stable noises. For $\alpha<2$, stationary states of the system described by Eq. (2) (if exist) are not of the Boltzmann-Gibbs type and can be multimodal. In particular, for $\alpha=1$, the stationary state is [17,72]

$$p_{\alpha=1}(x) = \frac{1}{\pi(1-x^2+x^4)}. \tag{9}$$

The nonzero asymmetry parameter β introduces asymmetry to stationary states [73]. This asymmetry can be measured by the ratio of the probability mass located at the left-hand side of the origin p_t(left),

$$p_t(\text{left}) = \text{Prob}\{x(t)<0\} = \int_{-\infty}^{0} p(x,t)dx = 1 - p_t(\text{right}). \tag{10}$$

The measure defined in Eq. (10) can be calculated also in time-dependent situations. For example, for the periodically modulated asymmetry parameter,

$$\beta = \beta_{\max}\sin\Omega t = \beta_{\max}\sin\left[\frac{2\pi}{T_{\Omega}}t\right]. \tag{11}$$

The periodic modulation of the asymmetry parameter results in the periodic modulation of the occupation fraction p_t(left). This in turn leads to the occurrence of the resonant effect—dynamical hysteresis. The strength of the effect can be characterized by the hysteresis loop area

$$\text{HL} = \int_{t=0}^{t=2\pi/\Omega} p_t(\text{left})d(\sin\Omega t). \tag{12}$$

In what follows, we study the dependence of the hysteresis loop area (HL) on the noise and driving parameters [see Eqs. (3) and (11)]. Due to the very complex form of the fractional Fokker-Planck equation (7), our studies are solely based on Eq. (1). Equation (1) provides an efficient method of constructing solutions to Eq. (7) which avoids instabilities of a numerical approximation to the fractional Fokker-Planck equation [74]. The Langevin equation (1) can be easily extended to time-dependent situations and more complex boundary conditions [63].

B. Results

Traditionally, stochastic resonance is studied in periodically modulated double-well potentials as a function of the noise intensity. Here, we study properties of the dynamical hysteresis, which is the manifestation of the stochastic resonance in the single-well fourth-order potential with the periodically modulated asymmetry parameter β as a function of the scale parameter (noise intensity) σ and the stability index α. The presence of the maximal area of a hysteresis loop indicates the occurrence of the stochastic resonance in the system at hand. Furthermore, the presented model provides a minimalistic setup in comparison to the standard double-well setup.

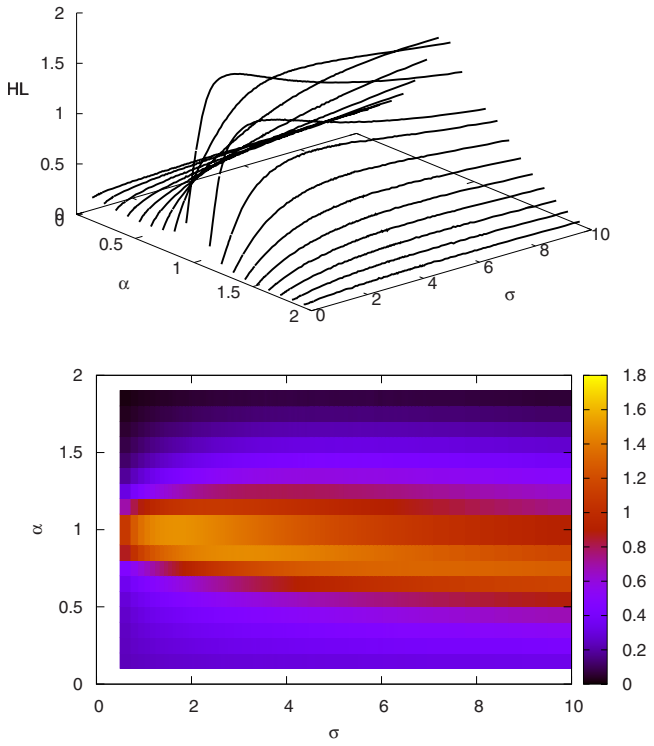

FIG. 2. (Color online) Area of the dynamical hysteresis loop HL [see Eq. (12)] as a function of the stability index α and the scale parameter (noise intensity) σ. Lower panel presents interpolated two-dimensional color map corresponding to the top panel (results for $\alpha=1$ are included only due to limitations of the graphic software). Equation (1) was numerically approximated with $\Delta t=10^{-3}$ and averaged over $N=10^5$ realizations. Other parameters are $\beta_{\max}=1$ and $T_{\Omega}=1$ [see Eq. (11)].

The hysteresis loop area is determined by two groups of factors. The first group of factors is connected to the characteristic features of noise pulses. This characteristic is controlled by the value of the stability index α and the scale parameter σ. The second group of factors is connected to the properties of periodic modulation of the asymmetry parameter β. Accordingly, the periodic modulation is characterized by the strength of the asymmetry parameter modulation $\beta_{\max}$ and the driving period T_{Ω}.

1. Role of the noise intensity and the stability index

Figure 2 presents the dependence of the hysteresis loop area as a function of the scale parameter σ and the stability index α for $\beta_{\max}=1$ and $T_{\Omega}=1$ demonstrating its nonmonotonous dependence on both parameters. Therefore, for a fixed value of the stability index α, it is possible to find such a value of the noise intensity σ for which the area of the hysteresis loop is maximal. Analogously, for a fixed value of the noise intensity σ, it is possible to find such a value of the

stability index α that maximizes the area of the hysteresis loop. Consequently, the observed resonant effect is of the double type.

The occurrence of hysteresis and nonmonotonous dependence of the hysteresis loop area originates from properties of stable densities. The nonzero noise asymmetry ($\beta \neq 0$) introduces the asymmetry of stationary states. The sinusoidal modulation of noise asymmetry periodically modulates the fraction p_t(left) of the probability mass located at one side of the origin. For $\alpha < 2$, stable densities are skewed into the direction determined by the sign of the asymmetry parameter (see Fig. 1). The size of asymmetry is controlled by the absolute value of the asymmetry parameter β giving rise to the strongest asymmetry for $|\beta|=1$. The further increase in asymmetry can be produced by the decrease in the stability index α. For $\alpha < 1$, with $|\beta|=1$, stable densities are totally skewed, i.e., stable random variables take values smaller (for $\beta=-1$) or larger (for $\beta=1$) than the location parameter μ. Such an extreme situation takes place only for $|\beta|=1$ with $\alpha < 1$. Otherwise, distributions are still skewed but the support of stable densities is not restricted. Therefore, noise pulses can be in any direction. The direction indicated by the asymmetry parameter is favored over the opposite directions.

The size of noise pulses is determined by the scale parameter σ and the stability index α. A decrease of the stability index α or an increase of the scale parameter σ increases the jump length experienced by a test particle. The different roles of the stability index α and the noise intensity σ are well visible for asymmetric noises when changes in α not only make tails heavier but also change the shape of distributions (see Fig. 1). In contrast, the increase in the value of the noise intensity σ increases the overall width of the distribution, i.e., it acts in the analogous way to the increase in temperature in systems driven by thermal noise [30,31].

The area of the hysteresis loop depends in a nonmonotonous way on the scale parameter σ. In the limit of the scale parameter $\sigma \to 0$, the particle tends to be located at the origin and the hysteresis is not observed. In the standard stochastic resonance, for $\sigma \to \infty$, the chance of long jumps is large enough to destroy the effect of the dynamical hysteresis. Here, the situation is different. A large value of the scale parameter σ leads to the better input-output synchronization (see Fig. 7) and consequently the area of the hysteresis loop decreases. Nevertheless, like in the classical stochastic resonance, there exists such an intermediate optimal value of the noise for which the system's response (measured by the hysteresis loop area) is maximal (see Fig. 3).

The area of the hysteresis loop is not only a nonmonotonous function of the noise intensity but also of the stability index α, i.e., at the system at hand, double stochastic resonance is observed. In the limit of small or large values of the stability index α, i.e., $\alpha \to 0$ or $\alpha \to 2$, the area of the hysteresis loop tends to zero. For $\alpha \to 0$, the decrease in the loop area is the consequence of heavy tails of stable distributions, i.e., for $\alpha \to 0$, tails of stable distributions become heavier and heavier. This in turn makes the test particle insensitive to the periodic modulation. For $\alpha \to 2$ with any value of the asymmetry parameter β, stable densities tend to the Gaussian distribution, which is intrinsically symmetric. Consequently, the hysteresis loop vanishes due to effective disappearance of periodic modulation (see Fig. 4).

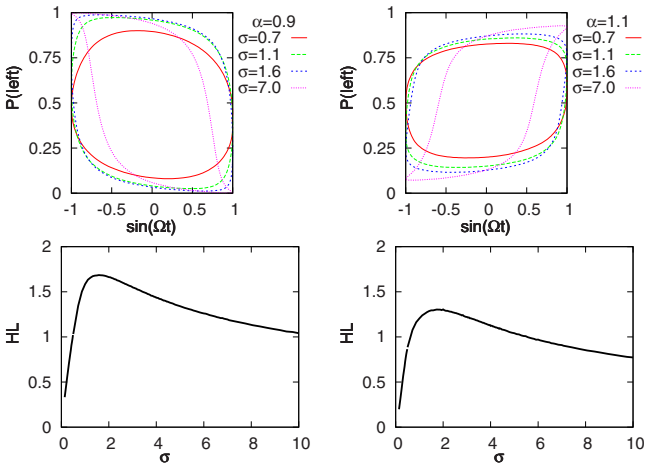

FIG. 3. (Color online) Sample hysteresis loops for $\sigma=\{0.7,1.1,1.6,7.0\}$ with $\alpha=0.9$ (left top panel) and $\alpha=1.1$ (right top panel). Dependence of the hysteresis loop area on the scale parameter (noise intensity) σ for $\alpha=0.9$ (left bottom panel) and $\alpha=1.1$ (right bottom panel). Simulation details as in Fig. 2.

Figure 3 presents sample cross sections of Fig. 2 for given values of the stability index α: $\alpha=0.9$ (left panel) and $\alpha=1.1$ (right panel) along with sample hysteresis loops. The top panel presents sample hysteresis loops for various values of noise intensity: $\sigma=\{0.7,1.1,1.6,7.0\}$ with $\alpha=0.9$ (top left panel) and $\alpha=1.1$ (top right panel). The bottom panel presents the dependence of the hysteresis loop area as a function of the noise intensity σ for $\alpha=0.9$ (bottom left panel) and $\alpha=1.1$ (bottom right panel).

Figure 4 presents sample cross sections of Fig. 2 for given values of the noise intensity σ: $\sigma=\sqrt{5}$ (left panel) and $\sigma=\sqrt{20}$ (right panel) along with sample hysteresis loops. The top panel presents sample hysteresis loops for various values of stability index: $\alpha=\{0.5,0.9,1.1,1.5\}$ with $\sigma=\sqrt{5}$ (top left panel) and $\sigma=\sqrt{20}$ (top right panel). The bottom panel presents the dependence of the hysteresis loop area on the sta-

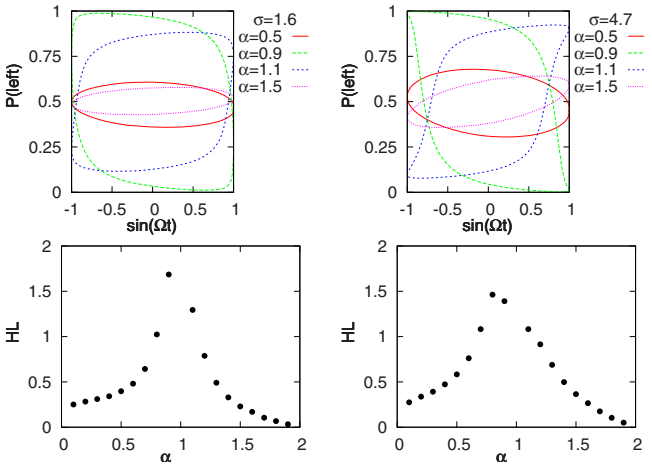

FIG. 4. (Color online) Sample hysteresis loops for $\alpha=\{0.5,0.9,1.1,1.5\}$ with $\sigma=\sqrt{5}$ (left top panel) and $\sigma=\sqrt{20}$ (right top panel). Dependence of the hysteresis loop area on the stability index α for $\sigma=\sqrt{5}$ (left bottom panel) and $\sigma=\sqrt{20}$ (right bottom panel). Simulation details as in Fig. 2.

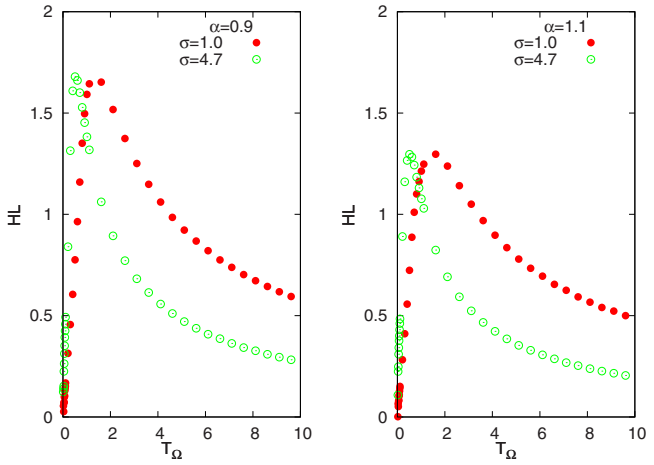

FIG. 5. (Color online) Area of the dynamical hysteresis loop HL [see Eq. (12)] as a function of the driving period T_Ω [see Eq. (11)] for $\alpha=0.9$ (left panel) and $\alpha=1.1$ (right panel). The value of the scale parameter σ is included in the figures' legends. Simulation details as in Fig. 2.

bility index α for $\sigma=\sqrt{5}$ (bottom left panel) and $\sigma=\sqrt{20}$ (bottom right panel).

The hysteresis loops visible in the top panels of Figs. 3 and 4 change their directions from clockwise ($\alpha<1$) to anticlockwise ($\alpha>1$). This phenomenon originates in properties of stable densities (see Fig. 1). On one hand, the sign of the asymmetry parameters indicates which tail of the stable distribution is heavier. On the other hand, for $\alpha<1$, stable densities can be one sided. These two properties determine the position of the modal value. More precisely, for $\alpha<1$ the modal value for $\beta=-1$ is located at the left-hand side of the origin, while for $\alpha>1$ it is located at the opposite side of the origin. The interchange of locations of modal values of stable densities with the increase in the stability index α from values smaller than 1 to values larger than 1 is responsible for the change in the directions of hysteresis loops (see Figs. 1, 3, and 4).

2. Role of the driving period and the asymmetry strength

The dynamical hysteresis occurs as a consequence of the delay in the system response to the external perturbation. On one hand, the increase in the period of modulation provides a test particle with a longer time to adapt to an updated set of noise parameters. Therefore, the increase in the period of modulation leads to the decrease in the hysteresis loop area. On the other hand, in the limit of very fast driving Ω the test particle feels the average value of the noise asymmetry β, i.e., effectively the driving noise is symmetric. Therefore, the area of the hysteresis loops tends to zero in the limit of fast driving. Consequently, as in the standard stochastic resonance, the area of the hysteresis loop depends in the nonmonotonous way on the value of the driving period T_Ω (see Fig. 5). For larger values of the scale parameter σ, the maximum of the hysteresis loop area is observed at smaller values of the driving period T_Ω (see Fig. 5).

The different effect has the decrease in the modulation strength, i.e., $\beta_{\max}$. With the decrease in $\beta_{\max}$ the decrease in the hysteresis loop area is observed. This effect originates as a consequence of the fact that smaller $\beta_{\max}$ decreases the asymmetry of the external driving (results not shown).

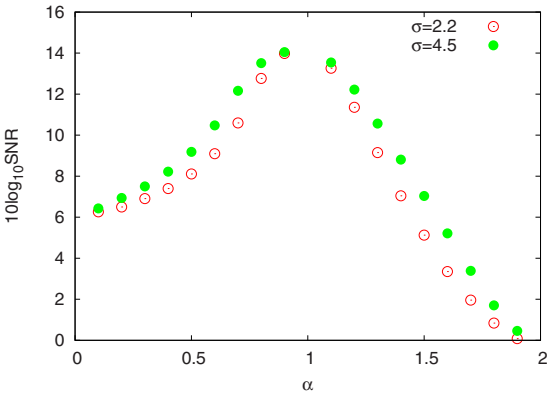

FIG. 6. (Color online) Signal-to-noise ratio (10 $\log_{10}$ SNR) as a function of the stability index α with $T_\Omega=1$ and $\sigma=\sqrt{5}$ or $\sigma=\sqrt{20}$. Simulation details as in Fig. 2.

3. Other measures of stochastic resonance

Traditionally, stochastic resonance is quantified by the signal-to-noise ratio, spectral power amplification, or periodic response [40,41]. However, studies performed here are based on the inspection of the dynamical hysteresis loop area [22,43,44,57]. Furthermore, the underlying process $x(t)$ [evolving in time according to Eq. (1)] is transformed to a two-state process by means of digital filtering [see Eq. (10)] and a further analysis examines the resulting two-state process. These two assumptions put some constraints on recorded findings.

Figure 6 presents signal-to-noise ratio curves corresponding to the hysteresis loop areas depicted in Fig. 4. From the signal-to-noise ratio curve, it is possible to find the optimal value of the stability index α corresponding to the maximal value of this quantifier. Both the hysteresis loop area and the signal-to-noise ratio indicate the same value of the optimal stability index α. Furthermore, in the middle panel of Fig. 7 p_t(left) corresponding to the signal-to-noise ratio is depicted, which indicates a nonmonotonous dependence of p_t(left) "amplitude" as a function of the stability index α. The nonmonotonous dependence of p_t(left) amplitude is captured by a nonmonotonous dependence of the hysteresis loop area (see Fig. 4) and the signal-to-noise ratio (see Fig. 6) as a function of the stability index α.

The signal-to-noise ratio as a function of the scale parameter σ or the driving period T_Ω does not behave in a nonmonotonous (rise and fall) way (results not shown). This can be deducted from the top and bottom panels of Fig. 7. The increase in the scale parameter σ or the driving period T_Ω leads to a better input-output synchronization. As a consequence, on one hand, the phase shift between the input signal and the system's response decreases, leading to a small hysteresis loop area (see Figs. 3 and 5). On the other hand, a better input-output synchronization leads to a larger value of the signal-to-noise ratio. Consequently, the signal-to-noise ratio is an increasing (smooth) function of the scale parameter σ

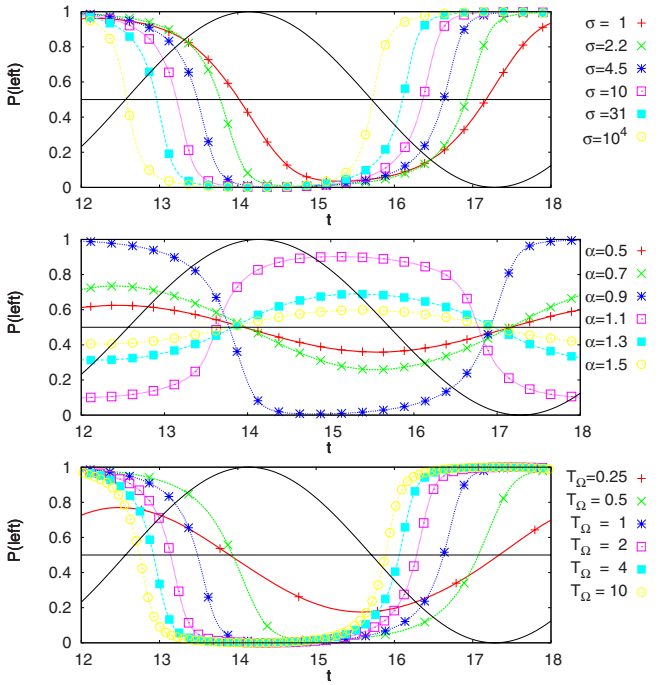

FIG. 7. (Color online) Time dependence of p_t(left): $\alpha=0.9$, $T_\Omega=1$ with various σ (top panel); $T_\Omega=1$, $\sigma=\sqrt{5}$ with various α (middle panel); and $\alpha=0.9$, $\sigma=\sqrt{20}$ with various T_Ω (bottom panel). Solid lines correspond to $0.5\sin(\Omega t)+0.5$ and 0.5 lines. Simulation details as in Fig. 2.

and increasing (fluctuating) function of the driving period T_Ω. Summarizing, other measures of the stochastic resonance (signal-to-noise ratio and spectral power amplification) could behave in a different manner than the hysteresis loop area, which indicates that special care is required in the inspection of the stochastic resonance.

III. SUMMARY AND CONCLUSIONS

Systems perturbed by white Lévy noises display a richer behavior than systems driven by white Gaussian noise. In particular, double stochastic resonance (as measured by the hysteresis loop area) can be observed in a single-well potential perturbed by Lévy stable noises without explicit external driving. Contrary to the standard studies of stochastic resonance, both the double-well potential and the external driving can be replaced with a periodic modulation of the asymmetry parameter characterizing a stable driving. A periodic modulation of the asymmetry parameter of the stable driving can mimic the presence of double-well potential and external periodic driving due to its nonequilibrium character. Qualitatively, the periodic modulation of the asymmetry parameter results in a periodic modulation of the effective potential, i.e., $V_{\mathrm{eff}}(x)\propto -\ln p(x)$, where $p(x)$ represents stationary density produced by the stable driving. This in turn lead to the occurrence of the dynamical hysteresis—the noise-induced effect manifesting the onset of the stochastic resonance.

Inspection of the hysteresis loop area confirms the double character of the observed stochastic resonance. In other words, the nonmonotonous dependence of the hysteresis loop area is observed both as a function of the scale parameter (noise intensity) and the stability index. More precisely, for a fixed value of the noise intensity, it is possible to find such a value of the stability index that maximizes the hysteresis loop area. Analogously, the same result can be achieved by fixing the stability index and varying the noise intensity. The effect of stochastic resonance disappears in the limit of zero noise intensity, extreme values of the stability index ($\alpha\to 0$ or $\alpha\to 2$), or extreme values of the periodic modulation ($T_\Omega\to 0$ or $T_\Omega\to\infty$). Furthermore, as in the classical stochastic resonance, the increase in the noise intensity weakens the effect measured by the hysteresis loop area.

ACKNOWLEDGMENTS

The research was supported by the Foundation for Polish Science and the Marie Curie TOK COCOS grant (6th EU Framework Program under Contract No. MTKD-CT-2004-517186). Fruitful suggestions from Ewa Gudowska-Nowak are greatly acknowledged.

[1] A. Janicki and A. Weron, *Simulation and Chaotic Behavior of α-Stable Stochastic Processes* (Marcel Dekker, New York, 1994).
[2] A. Janicki, *Numerical and Statistical Approximation of Stochastic Differential Equations with Non-Gaussian Measures* (Hugo Steinhaus Centre for Stochastic Methods, Wrocław, 1996).
[3] Y. L. Klimontovich, *Statistical Physics of Open Systems* (Kluwer Academic Publishers, Holland, 1994).
[4] *Lévy Flights and Related Topics in Physics*, edited by M. F. Shlesinger, G. M. Zaslavsky, and J. Frisch (Springer Verlag, Berlin, 1995).
[5] A. V. Chechkin, V. Y. Gonchar, and M. Szydłowski, Phys. Plasmas **9**, 78 (2002).
[6] M. A. Lomholt, T. Ambjörnsson, and R. Metzler, Phys. Rev. Lett. **95**, 260603 (2005).
[7] I. M. Sokolov, J. Mai, and A. Blumen, Phys. Rev. Lett. **79**, 857 (1997).
[8] E. Pereira, J. M. G. Martinho, and M. N. Berberan-Santos, Phys. Rev. Lett. **93**, 120201 (2004).
[9] P. D. Ditlevsen, Geophys. Res. Lett. **26**, 1441 (1999).
[10] P. D. Ditlevsen, M. S. Kristensen, and K. K. Andersen, J. Clim. **18**, 2594 (2005).
[11] P. Santini, Phys. Rev. E **61**, 93 (2000).
[12] G. M. Viswanathan *et al.*, Nature (London) **381**, 413 (1996).
[13] D. W. Sims *et al.*, Nature (London) **451**, 1098 (2008).
[14] A. M. Edwards *et al.*, Nature (London) **449**, 1044 (2007).
[15] N. Periasamy and A. Verkman, Biophys. J. **75**, 557 (1998).
[16] T. H. Solomon, E. R. Weeks, and H. L. Swinney, Phys. Rev. Lett. **71**, 3975 (1993).

[17] A. V. Chechkin, V. Y. Gonchar, J. Klafter, and R. Metzler, Adv. Chem. Phys. **133**, 439 (2006).
[18] R. Metzler, A. V. Chechkin, V. Y. Gonchar, and J. Klafter, Chaos, Solitons Fractals **34**, 129 (2007).
[19] B. Dybiec and E. Gudowska-Nowak, New J. Phys. **9**, 452 (2007).
[20] A. A. Dubkov, B. Spagnolo, and V. V. Uchaikin, Int. J. Bifurcation Chaos Appl. Sci. Eng. **18**, 2649 (2008).
[21] R. Klages, G. Radons, and I. M. Sokolov, *Anomalous Transport: Foundations and Applications* (Wiley-VCH, Weinheim, 2008).
[22] B. Dybiec and E. Gudowska-Nowak, J. Stat. Mech.: Theory Exp. **2009**, P05004.
[23] M. Perc, Phys. Rev. E **75**, 022101 (2007).
[24] M. Perc, Econ. Lett. **97**, 58 (2007).
[25] R. N. Mantegna and H. E. Stanley, *An Introduction to Econophysics: Correlations and Complexity in Finance* (Cambridge University Press, Cambridge, England, 2000).
[26] J. L. Cabrera and J. G. Milton, Chaos **14**, 691 (2004).
[27] H. K. Janssen, K. Oerding, F. van Wijland, and H. J. Hilhorst, Eur. Phys. J. B **7**, 137 (1999).
[28] B. Dybiec, A. Kleczkowski, and C. A. Gilligan, J. R. Soc., Interface **6**, 941 (2009).
[29] A. M. Reynolds and C. J. Rhodes, Ecology **90**, 877 (2009).
[30] L. Gammaitoni, P. Hänggi, P. Jung, and F. Marchesoni, Rev. Mod. Phys. **70**, 223 (1998).
[31] V. S. Anishchenko, A. B. Neiman, F. Moss, and L. Schimansky-Geier, Sov. Phys. Usp. **42**, 7 (1992).
[32] J. M. G. Vilar and J. M. Rubí, Phys. Rev. Lett. **78**, 2882 (1997).
[33] M. Perc, Phys. Rev. E **78**, 036105 (2008).
[34] Q. Wang, M. Perc, Z. Duan, and G. Chen, Chaos **19**, 023112 (2009).
[35] P. Hänggi, P. Talkner, and M. Borkovec, Rev. Mod. Phys. **62**, 251 (1990).
[36] C. R. Doering and J. C. Gadoua, Phys. Rev. Lett. **69**, 2318 (1992).
[37] V. S. Anishchenko and A. B. Neiman, in *Stochastic Dynamics*, edited by L. Schimansky-Geier and T. Pöshel (Springer Verlag, Berlin, 1997), p. 155.
[38] R. Rozenfeld, J. A. Freund, A. Neiman, and L. Schimansky-Geier, Phys. Rev. E **64**, 051107 (2001).
[39] N. V. Agudov and B. Spagnolo, Phys. Rev. E **64**, 035102(R) (2001).
[40] L. Gammaitoni, F. Marchesoni, and S. Santucci, Phys. Rev. Lett. **74**, 1052 (1995).
[41] F. Marchesoni, L. Gammaitoni, F. Apostolico, and S. Santucci, Phys. Rev. E **62**, 146 (2000).
[42] P. Talkner *et al.*, New J. Phys. **7**, 14 (2005).
[43] M. C. Mahato and S. R. Shenoy, Phys. Rev. E **50**, 2503 (1994).
[44] M. C. Mahato and A. M. Jayannavar, Phys. Rev. E **55**, 6266 (1997).
[45] B. McNamara, K. Wiesenfeld, and R. Roy, Phys. Rev. Lett. **60**, 2626 (1988).
[46] G. Giacomelli, F. Marin, and I. Rabbiosi, Phys. Rev. Lett. **82**, 675 (1999).
[47] D. Babič, C. Schmitt, I. Poberaj, and C. Bechinger, EPL **67**, 158 (2004).
[48] S. M. Bezrukov and I. Vodyanoy, Nature (London) **385**, 319 (1997).
[49] A. Fuliński, Phys. Rev. E **52**, 4523 (1995).
[50] R. D. Astumian and F. Moss, Chaos **8**, 533 (1998).
[51] P. Hänggi, ChemPhysChem **3**, 285 (2002).
[52] P. Hänggi, G. Schmid, and I. Goychuk, Nova Acta Leopold. **88**, 17 (2003).
[53] P. Jung, G. Gray, R. Roy, and P. Mandel, Phys. Rev. Lett. **65**, 1873 (1990).
[54] M. C. Mahato and A. M. Jayannavar, Physica A **248**, 138 (1998).
[55] M. Evstigneev, P. Reimann, C. Schmitt, and C. Bechinger, J. Phys.: Condens. Matter **17**, S3795 (2005).
[56] J. Juraszek, B. Dybiec, and E. Gudowska-Nowak, Fluct. Noise Lett. **5**, L259 (2005).
[57] B. Dybiec and E. Gudowska-Nowak, Acta Phys. Pol. B **38**, 1759 (2007).
[58] W. Feller, *An Introduction to Probability Theory and Its Applications* (John Wiley, New York, 1968).
[59] A. Weron and R. Weron, Lect. Notes Phys. **457**, 379 (1995).
[60] R. Weron, Stat. Probab. Lett. **28**, 165 (1996).
[61] B. Dybiec and E. Gudowska-Nowak, Phys. Rev. E **69**, 016105 (2004).
[62] B. Dybiec and E. Gudowska-Nowak, Fluct. Noise Lett. **4**, L273 (2004).
[63] B. Dybiec, E. Gudowska-Nowak, and P. Hänggi, Phys. Rev. E **73**, 046104 (2006).
[64] B. Dybiec, E. Gudowska-Nowak, and P. Hänggi, Phys. Rev. E **75**, 021109 (2007).
[65] H. C. Fogedby, Phys. Rev. E **58**, 1690 (1998).
[66] R. Metzler, E. Barkai, and J. Klafter, EPL **46**, 431 (1999).
[67] V. V. Yanovsky, A. V. Chechkin, D. Schertzer, and A. V. Tur, Physica A **282**, 13 (2000).
[68] D. Schertzer *et al.*, J. Math. Phys. **42**, 200 (2001).
[69] A. A. Dubkov and B. Spagnolo, Fluct. Noise Lett. **5**, L267 (2005).
[70] A. A. Dubkov and B. Spagnolo, Acta Phys. Pol. B **38**, 1745 (2007).
[71] I. Podlubny, *Fractional Differential Equations* (Academic Press, San Diego, 1998).
[72] A. V. Chechkin *et al.*, J. Stat. Phys. **115**, 1505 (2004).
[73] B. Dybiec, E. Gudowska-Nowak, and I. M. Sokolov, Phys. Rev. E **76**, 041122 (2007).
[74] M. M. Meerschaert and C. Tadjeran, J. Comput. Appl. Math. **172**, 65 (2004).